

FOS Spectropolarimetry

A. Storrs, A. Koratkar, C. Keyes, H. Bushouse, M. De La Peña, and R. Allen
May 1998

ABSTRACT

This is the comprehensive closeout ISR on FOS spectropolarimetry. The various sections of this document contain the detailed theory of spectropolarimetry with the FOS, including the correction for COSTAR-induced polarization, a discussion of the format of the FOS polarimetry files, a description of how to manipulate the data with the STSDAS spec_polar package, and a discussion of the accuracy of the calibration, which at the 1σ level is about 0.3 percent for linear polarization pre-COSTAR and 0.5 percent post-COSTAR. How the post-COSTAR polarization files (PCP files) are made and how the recalibration of archived data has been conducted, as well as a summary of general conclusions are also presented. An appendix containing the IRAF script used in producing the PCP files is included for completeness.

This report encompasses a variety of topics that are of interest to a broad spectrum of users. To help you find information, we list the major sections of this document:

- Instrument Description and FOS Polarimetry Principles (page 2)
- FOS Data Formats and Output Data (page 8)
- Re-Calibration and Data Analysis (page 13)
- FOS Polarimetry Calibration Accuracies (page 16)
- COSTAR Polarization Correction (page 20)
- Summary of Re-archival of Re-calibrated FOS Polarimetry Data (page 22)
- Conclusions and Recommendations (page 22)
- References (page 23)
- Appendix (page 23)

1. Instrument Description and FOS Polarimetry Principles¹

Polarization measurements are a powerful tool for astronomers, especially useful for studying some of the more extreme phenomena. Radiation originating in regions of magnetic field is often linearly or circularly polarized. The Zeeman effect, synchrotron and cyclotron emission are well known. Scattering processes in asymmetric geometry also cause linear polarization. Resonance scattering, electron scattering, and dust scattering often modify light on its way from the source of emission, leaving clues in the polarization. We can use these clues to study phenomena as diverse as the composition and shape of dust grains a few hundred Å across, to the brilliant emission coming from the edge of very massive black holes in the nuclei of galaxies.

The object of spectropolarimetric observations is to determine the magnitude of the Stokes vectors I, Q, U, and V at different wavelengths. These are sometimes called “Stokes spectra”.

I is the intensity of the light:

$$I = I_0 + (Q^2 + U^2 + V^2)^{1/2}$$

(where I_0 is the unpolarized intensity), Q and U define the linear polarization P:

$$P = (Q^2 + U^2)^{1/2} / I$$

and V defines the circular polarization:

$$P_c = V / I$$

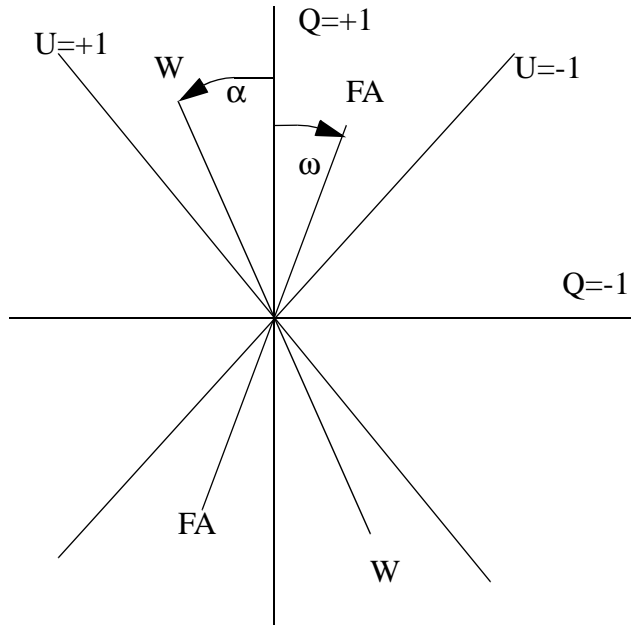
The angle of the linear polarization is θ :

$$\theta = 1/2 \tan^{-1}(U/Q)$$

The coordinate system used in this analysis is shown in Figure 1. Note that this is the instrumental coordinate system, that is circular polarization V is defined as positive for a clockwise rotation of the E-vector, and $U=+1$ is 45° counter-clockwise from the $Q=+1$ axis. This convention is used because we are examining the polarization from the instrument’s point of view, not from the source’s as is more common in physics texts.

1. Most of this section is adapted from Allen and Angel 1982, and Allen 1995.

Figure 1: Coordinate system used in the polarization analysis. The view is toward the source. The line W-W is the pass direction of the Wollaston prism, while FA-FA is the fast axis of the waveplate. W-W is at an angle α from the Q=+1 axis, while FA-FA is at an angle ω from that axis.



The FOS Spectropolarimeter

The technique used for spectropolarimetry in the FOS is very similar to that developed for ground-based instruments. A polarizing prism of doubly refractive material was introduced into the spectrophotometer, so as to form two images of the slit in opposite senses of polarization at the detector. These two images are the two pass directions referred to in the FOS literature. The polarizing element was left fixed, and a waveplate was introduced ahead of it which was turned to analyze linear and circular polarization. In this way polarization effects in the dispersing optics following the analyzing prism were of no consequence, and had no effect on the accuracy of the measurement.

There were two polarization analyzer elements available in the FOS: a thick waveplate (plate "A") plus Wollaston prism assembly, and a thin waveplate plus Wollaston prism assembly (plate "B"). The waveplate+prism assemblies rotated in order to observe the spectra from both pass directions at different position angles. In normal spectropolarimetry, to correctly determine the linear and circular polarization properties of the incoming beam, each spectrum was observed once at each of 4, 8, or 16 position angles of the waveplate relative to the Wollaston prism. The waveplate could be rotated through any desired angle, but in the standard mode the position angles were separated by 22.5 degrees.

The two undispersed polarized beams were further separated and redirected onto an off-axis collimator by a roof-shaped grazing-incidence mirror. The collimator directed the

light onto the grating/filter wheel. The concave gratings of the filter/grating wheel dispersed the light and re-imaged it onto a Digicon detector.

In the pre-COSTAR era, the polarimeter could be used with either the red or blue detectors of the FOS. Only the 4.3 aperture was calibrated pre-COSTAR and only the 1.0 aperture was calibrated post-COSTAR (see Table 1). In the post-COSTAR era, however, FOS/BL was preferred because of lower geomagnetically induced image motion (GIM) and lower instrumental polarization. A schematic of the instrumental setup is shown in Figure 2. Note that only the G130H, G190H, G270H, and G400H gratings were ever calibrated

Figure 2: Schematic of FOS spectropolarimeter setup. Light enters from the top and ultimately forms two spectra on the photocathode. The retardation (phase shift between the two polarized rays) of the waveplate at any given wavelength is δ .

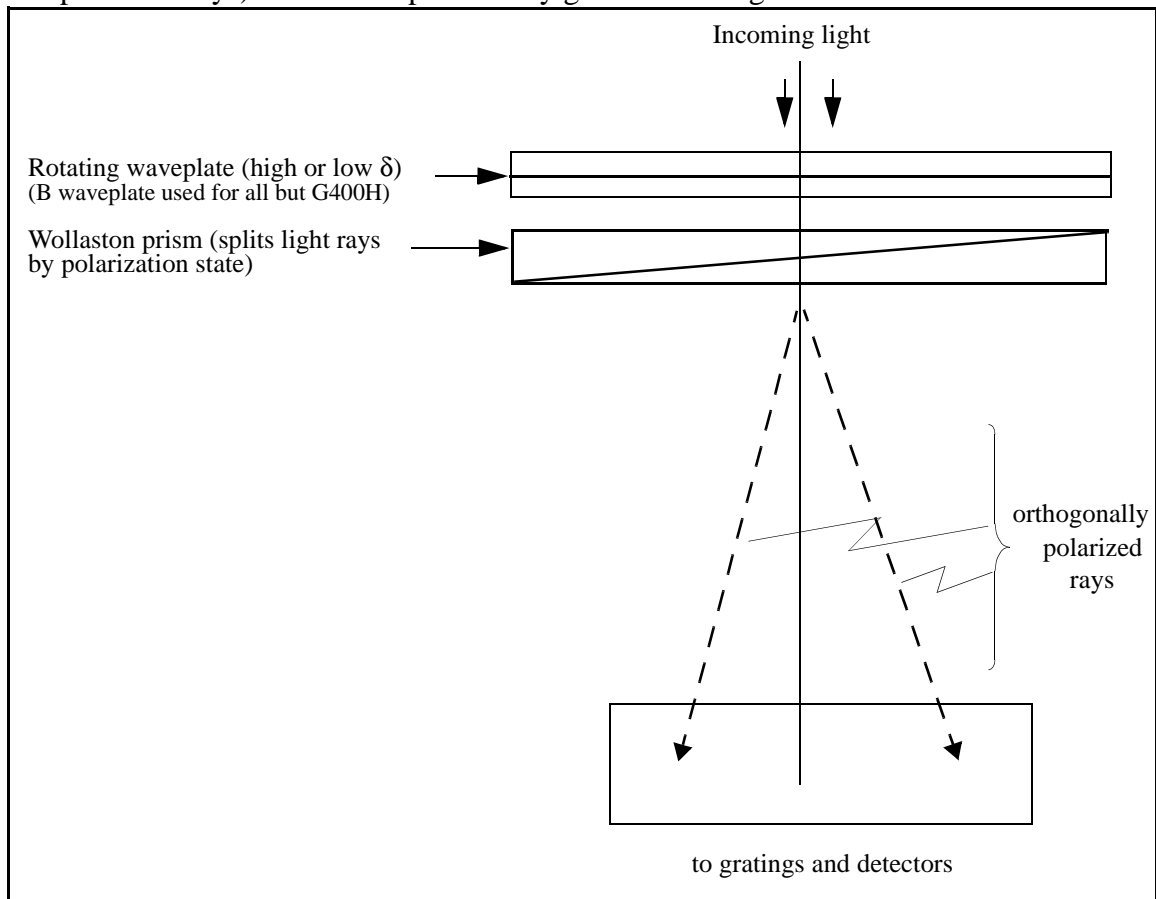


Table 1. Calibrated Modes

Side	Grating	Pre-COSTAR	Post-COSTAR
		Aperture	Aperture
FOS/BL	G130H	4.3	—
	G190H	4.3	1.0
	G270H	4.3	1.0
	G400H	—	1.0
FOS/RD	G190H	4.3	—
	G270H	4.3	—

Details of the calculations:

An incoming beam with Stokes spectra I, Q, U, and V are analyzed by the waveplate (at angle ω from the Q=+1 axis, and retardation δ) so that at a given wavelength the detected Stokes spectra I', Q', U', and V' will be:

$$I' = I \quad \text{Eq. 1}$$

$$Q' = Q\left(\frac{1}{2}(1 + \cos\delta) + \frac{1}{2}(1 - \cos\delta)\cos 4\omega\right) - U\left(\frac{1}{2}(1 - \cos\delta)\sin 4\omega\right) + V(\sin\delta\sin 2\omega) \quad \text{Eq. 2}$$

$$U' = -Q\left(\frac{1}{2}(1 - \cos\delta)\sin 4\omega\right) + U\left(\frac{1}{2}(1 + \cos\delta) - \frac{1}{2}(1 - \cos\delta)\cos 4\omega\right) + V(\sin\delta\cos 2\omega) \quad \text{Eq. 3}$$

$$V' = -Q(\sin\delta\sin 2\omega) - U(\sin\delta\cos 2\omega) + V\cos\delta \quad \text{Eq. 4}$$

With the Wollaston at an angle α from the Q=+1 axis, the signal detected will be:

$$J = \frac{1}{2}(I' + Q'\cos 2\alpha + U'\sin 2\alpha) \quad \text{Eq. 5}$$

If the system is aligned so that $\alpha=0^\circ$, we can substitute eqs. 1-4 to get:

$$J'_i = \frac{I}{2} + \frac{Q}{4}(1 + \cos\delta) + \frac{Q}{4}(1 - \cos\delta)\cos 4\omega - \frac{U}{4}(1 - \cos\delta)\sin 4\omega + \frac{V}{2}(\sin\delta\sin 2\omega) \quad \text{Eq. 6}$$

for the $\alpha=0^\circ$ axis ray from the Wollaston, and

$$J''_i = \frac{I}{2} - \frac{Q}{4}(1 + \cos\delta) - \frac{Q}{4}(1 - \cos\delta)\cos 4\omega + \frac{U}{4}(1 - \cos\delta)\sin 4\omega - \frac{V}{2}(\sin\delta\sin 2\omega) \quad \text{Eq. 7}$$

for the $\alpha=90^\circ$ axis ray. The subscript i corresponds to the rotation position of the waveplate.

The functional dependence of J on ω in equations 6 and 7 shows that a rotating waveplate in front of an analyzer will modulate a linearly polarized beam at 4 times the rotation

rate, while a circularly polarized beam will be modulated at 2 times the rotation rate. These equations also show that if the retardation δ is known, measures of J as a function of ω can be used to determine the Stokes parameters I , Q , U , and V of the source. *In practice, the use of only four waveplate positions did not uniquely determine the circular polarization.* Especially in the post-COSTAR era this measurement is of great interest, as discussed below.

COSTAR introduced two reflections in front of the polarimeter. The polarization state of the incoming light was altered by the fact that the COSTAR mirrors have different reflectivities for light vibrating parallel and perpendicular to the line of centers between the mirrors. Since the parallel vibrations were also shifted in phase relative to the perpendicular vibrations, some incoming linear polarization was converted to circular polarization, and vice versa. Fortunately the effects of these mirrors could be determined from observations of unpolarized and polarized standard stars. Observations of an unpolarized standard provided relative measures of the parallel and perpendicular reflectivities, while observations of a polarized standard could be used to determine the phase shift. The polarization of an unknown source can then be recovered by numerically inverting the reflection process.

In Mueller matrix formulation, the output polarized beam S' (consisting of the observed Stokes spectra I' , Q' , U' , and V') after being reflected off of a mirror with angle ρ between the mirror normal and the incoming $Q=+1$ axis is:

$$S' = M(\rho) \bullet S$$

where S is the input (polarized) beam. But

$$M(\rho) = T(-\rho) \bullet M(0) \bullet T(\rho)$$

where the rotation matrix $T(\rho)$ is:

$$T(\rho) = \begin{bmatrix} 1 & 0 & 0 & 0 \\ 0 & \cos 2\rho & \sin 2\rho & 0 \\ 0 & -\sin 2\rho & \cos 2\rho & 0 \\ 0 & 0 & 0 & 1 \end{bmatrix}$$

and $M(0)$ is

$$M(0) = \begin{bmatrix} 0.5(r_p + r_s) & 0.5(r_p - r_s) & 0 & 0 \\ 0.5(r_p - r_s) & 0.5(r_p + r_s) & 0 & 0 \\ 0 & 0 & \sqrt{r_p r_s} \cos \delta & \sqrt{r_p r_s} \sin \delta \\ 0 & 0 & (-\sqrt{r_p r_s}) \sin \delta & \sqrt{r_p r_s} \cos \delta \end{bmatrix}$$

where r_p is the parallel reflection coefficient, and r_s the perpendicular.

When $\rho=0$ and $Q=U=V=0$, as is the case with an unpolarized standard, the output Stokes vectors reduce to

$$I' = 0.5 (r_p + r_s) I$$

$$Q' = 0.5 (r_p - r_s) I$$

$$U' = 0$$

$$V' = 0$$

Thus $r_p/r_s = (1+Q'/I')/(1-Q'/I')$, showing that the reflection ratio can be measured from observations of an unpolarized source. Since the flux of the standard is known ahead of time, there is no need to find separate values for r_p and r_s .

Measurements of the phase shift required a polarized standard and were a little more complicated. When $\rho = 0$ and $V = 0$, the output Stokes vectors are:

$$I' = 0.5 (r_p + r_s) I + 0.5 (r_p - r_s) Q$$

$$Q' = 0.5 (r_p - r_s) I + 0.5 (r_p + r_s) Q$$

$$U' = \sqrt{r_p r_s} (\cos \delta) U$$

$$V' = -\sqrt{r_p r_s} (\sin \delta) U$$

Thus the phase shift is $\delta = -\arctan(V'/U')$. As can be seen from this formula, the phase shift required measuring both U and V . It was therefore critical that the polarized standard had its linear polarization precisely $+45^\circ$ or -45° to the plane of incidence of the COSTAR mirrors, so that the condition $V=0$ was satisfied and U' and V' could be accurately measured.

Corrections to the Stokes vectors of an unknown source are done by numerically passing the observed values of I' , Q' , U' , and V' through an inverse mirror reflection. In this reflection, the perpendicular reflection coefficient r_s is taken to be 1.0, the parallel reflection coefficient r_p is set equal to $(1+Q'/I')/(1-Q'/I')$ (where Q' and I' are measured from an unpolarized standard), and the phase shift is set equal to $\arctan(V'/U')$ (where V' and U'

are in this case measured from a polarized source). Except for a flux factor, all of the Stokes vectors are recovered in this process. Errors are derived from the coefficients of the mirror matrix and the statistical uncertainties in the original measurements. Since the corrections are based solely on relations that apply when $\rho=0$, the observational Stokes vectors have to be corrected in a frame that has $Q=1$ in the plane of incidence of the mirrors. This means that a rotation to the $Q=1$ frame, a correction for COSTAR, and another rotation to the plane of the sky frame are required to get the final values in the frame of the sky.

Although the correction scheme outlined here is particularly straightforward, actual observations show that there was a small amount of wavelength dependent U present even when the reductions are done in a coordinate system that was aligned with the line of centers between the mirrors. While this suggests that the COSTAR mirrors do not have identical reflectivities and do not share a common plane of incidence, a satisfactory correction scheme has been adopted in which the U contribution was removed before any subsequent steps in the processing. Note that the correction for COSTAR-induced phase shift required knowing the circular polarization. *Thus only data with POLSCAN= 8 or 16 can be adequately corrected for the effects of the COSTAR mirrors.*

2. FOS Data Formats and Output Data

The waveplate plus Wollaston prism assemblies were located just behind the entrance apertures of the FOS and split the incoming beam into a pair of spectra that correspond to orthogonal directions of polarization. The first spectrum was of the first pass direction, and the second of the other pass direction (see Figure 2). One FOS exposure was composed of an observation of each of these two spectra and was accomplished by alternately deflecting the spectra onto the diode array. The raw dataset (.d0h headers) for an FOS observation contains the two spectra observed at each waveplate position angle stored sequentially in a single data group of the multigroup images. Thus for a quarter-stepped spectrum, consisting of 2064 pixels, each data group in the .d0h images has 2 x 2064 pixels of data; pixels 1–2064 contain the spectral data for pass direction 1, while pixels 2065–4128 contain the spectral data for pass direction 2. The number of data groups in a raw (.d0h) image is usually equal to the number of different waveplate position angles (usually 4, 8, or 16) at which observations were obtained for the spectral pairs. Long exposures (e.g., on near-CVZ targets) might have multiple groups for a given waveplate angle. The header parameter NREAD gives the number of group readouts—it may be greater than one in this case. The quantities stored in groups after the first, always are the accumulated results of all groups to that point. The last group always contains the results for the entire exposure.

The raw datasets for polarimetry observations follow the normal calibration process provided by the task **calfos**. The basic reduction steps include conversion from counts to

count rates (i.e., division of the spectra by the exposure time), corrections for detector non-linearities, subtracting background from the object spectra, flatfielding the object spectra, and converting the countrate object spectra to absolute flux units. Statistical errors in the object spectra—computed as the square-root of the original number of counts per pixel—are also propagated through each of these operations without further error propagation (in IRAF, type “help calfos” for more details of the routine calibration process). After the completion of the generic calibration processing steps outlined above, the **calfos** procedure applies extra steps of processing that are unique to spectropolarimetry datasets (indicated by the header parameter MOD_CORR being set to PERFORM).

Note that during cycle 6, the “average inverse sensitivity” (AIS) calibration procedure was installed in **calfos**. While this is the recommended procedure for recalibration of *non-polarimetric* FOS spectroscopy data taken in any cycle, AIS calibration reference files for polarimetry observations have not been generated. Thus FLX_CORR should be set to PERFORM, and AIS_CORR, APR_CORR, and TIM_CORR should be set to OMIT in the raw (.d0h) header before running **calfos**.

After the completion of generic calibrations steps in **calfos** there are four images in the calibrated dataset that are of interest to the analysis of polarimetric data: the wavelength image, with an image name extension of .c0h, the flux-calibrated object spectra image, with an extension of .c1h, the flux-calibrated statistical errors image, with an extension of .c2h, and the data quality flags image, with an extension of .cqh. The formats of these calibrated images are rearranged somewhat relative to the format of the original raw (.d0h) image. Instead of having the two spectra (pass direction 1 and pass direction 2) obtained at each waveplate position stored back-to-back in a single data group, they are stored sequentially in pairs of individual groups where each group is now only 2064 pixels in length. The spectra from pass direction 1 are stored in the odd-numbered groups, while the pass direction 2 spectra are in the even-numbered groups. A one-to-one correspondence is maintained between the groups in the wavelength (.c0h), flux (.c1h), error (.c2h), and data quality (.cqh) images. For example, the wavelength vector in group 3 of the .c0h image is to be associated with the flux spectrum in group 3 of the .c1h image, as are the error spectra and data quality vectors in group 3 of the .c2h and .cqh images, respectively.

Wavelength Image (.c0h)

This image consists of 2*POLSCAN groups with wavelengths for both pass directions through the Wollaston prism and each waveplate position. The wavelengths for the different waveplate positions should be identical (rotating the waveplate does not shift the spectra), but the wavelengths are offset by a constant amount between the two pass directions at each waveplate position. Therefore the wavelength vectors contained in the odd-numbered groups of a .c0h image will all be identical, as will the wavelengths in the

even-numbered groups, but there is a constant offset between the values in the odd- and even-numbered groups.

Flux Image (.c1h)

This image with 2*POLSCAN groups contains the calibrated flux spectra for both pass directions through the Wollaston prism and each waveplate position. The relationship between image group number, pass direction, and waveplate position is as outlined above for the wavelength image. Note that unlike calibrated flux data for non-polarimetric observations, the first group will not represent the total absolute flux for the source, but only half. Representative fluxes are formed by averaging the fluxes from the set of waveplate positions for each pass direction separately and then summing the two. However, as discussed above, there is a wavelength shift between the spectra from the two pass directions. To combine the two mean spectra from both pass directions one of them must be shifted to align with the other (use **imshift** in **iraf.images** or **resample** in **stdas.hst_calib.ctools**) and then sum the two spectra. However the total flux (Stokes I) is also computed by the spectropolarimetric reduction process (in the .c3h image; see below) and the shift handled automatically by **calfos**, the total flux is more conveniently accessed there.

Statistical Error Image (.c2h)

An image with 2*POLSCAN groups representing statistical error on the calibrated flux for both pass directions through the Wollaston prism and each waveplate position. The flux error spectra are stored in exactly the same fashion as the wavelength and flux spectra. As is the case with the calibrated flux data, this data set differs from the statistical errors for non-polarimetric data in that the errors cannot be simply combined. It is suggested that the error on Stokes I computed by the polarimetric processing be used for the total flux error.

Data Quality Image (.cqh)

An image with 2*POLSCAN groups containing data quality values for the calibrated fluxes. The organization is exactly the same as that of the calibrated fluxes. The data quality values are as follows:

Table 2. Data quality values

DQ Value	Condition
50	Sampling less than 50% of nominal
100	Reed-Solomon decoding error
120	Sky or background spectrum repaired or extrapolated
130	Moderate saturation correction (uncertainty > 5%)
160	Possible contamination from intermittent dead diode
170	Possible contamination from intermittent noisy diode
190	Large saturation correction (uncertainty > 20%)
200	Invalid inverse sensitivity value applied
300	Severe saturation correction (uncertainty > 50%)
400	Disabled diode
700	Data filled due to ground-based GIMP correction
800	Data filled

Polarimetry Image (.c3h)

Using the calibrated wavelength, flux, error, and data quality spectra, **calfos** performs the spectropolarimetric processing in the following five steps:

1. Compute Stokes parameter IQUV spectra and errors, as well as linear polarization (PL), polarization position angle (THETA), and circular polarization (PC), and their associated errors, for spectra from pass direction 1;
2. Compute Stokes parameter IQUV spectra and errors, as well as linear polarization (PL), polarization position angle (THETA), and circular polarization (PC), and their associated errors, for spectra from pass direction 2;
3. Compute the weighted mean of the Stokes IQUV spectra (and errors) from the two pass directions, and recompute PL, THETA, and PC (and errors) from the mean Stokes spectra;
4. Determine if the data was obtained post-COSTAR, and if so, apply the corrections discussed in section 1;
5. Correct the mean Stokes and polarization spectra computed in step 3 for interference between Q and U and correct THETA for instrumental orientation (i.e. transform THETA from instrumental coordinates to sky coordinates).

The results of the polarimetric processing are stored in the so-called “special statistics” file, which has the same root file name as the rest of the dataset with an image name extension of .c3h. The .c3h image contains 56*NREAD data groups (see Table 3), organized as follows: For each readout (NREAD), four sets of 14 groups, with the first set (groups 1–14) containing polarization spectra associated with pass direction 1, the second set (groups 15–28) containing polarization spectra for pass direction 2, the third set (groups 29–42) containing polarization spectra for both pass directions merged, and the fourth set (groups 43–56) containing the combined polarization spectra that have been corrected for interference and instrument orientation on the sky. The organization of each set of 14 groups is as follows:

Table 3. .c3 (calibrated polarimetry) file structure

Set 1 Pass dir 1	Set 2 Pass dir. 2	Set 3 Pass dir. 1+2	Set 4 Pass dir. 1+2+corr.	Contents
Group 1	Group 15	Group 29	Group 43	Stokes I
2	16	30	44	Stokes Q
3	17	31	45	Stokes U
4	18	32	46	Stokes V
5	19	33	47	Stokes I error
6	20	34	48	Stokes Q error
7	21	35	49	Stokes U error
8	22	36	50	Stokes V error
9	23	37	51	Lin. pol. (PL)
10	24	38	52	Circ. pol. (PC)
11	25	39	53	Pol. PA (θ)
12	26	40	54	PL error
13	27	41	55	PC error
14	28	42	56	θ error

The fourth set of Stokes and polarization spectra (corresponding to the merged and corrected data) is normally the one of interest for further science analysis.

The wavelength assignments for the first set of polarization spectra (groups 1–14) in the .c3h image are the same as that of the flux spectra for the first pass direction, which is contained in group 1 of the .c0h image. The wavelength assignments for set 2 (groups 15–28) of the .c3h image are the same as that for the flux spectra for pass direction 2, which is contained in group 2 of the .c0h image. *For the combined data contained in the*

third and fourth sets (groups 29-56) of the .c3h image, the wavelengths are the same as that of the first pass direction, and therefore are again given by group 1 of the .c0h image.

Remember, the last set of 56 groups contains the results for an entire accumulated exposure.

The data quality values contained in the .cqh image only strictly apply to each of the individual flux spectra contained in the .c1h image. Because the polarization spectra in the .c3h image are computed from the combination of all flux spectra, there is no longer a one-to-one correspondence between any of the individual data quality vectors in the .cqh image and the polarization spectra. The data quality values are used to exclude individual bad pixels in the flux spectra during the process of computing the polarization spectra; any pixel with a data quality value of 200 or greater is not used in the computation of polarimetry values at that channel. In the event that there are fewer than four good (non-rejected) input flux values at a given channel, the output Stokes and polarization values (and errors) for that channel are set to zero. *Bad pixels in the .c3h image can therefore be identified by the fact they have error values equal to zero.* A value of zero for one of the polarization quantities by itself does not necessarily constitute a bad pixel since zero can be a physically-meaningful value for flux or polarization. Only if the associated error value is equal to zero can we safely conclude that this is a bad pixel and should be ignored.

3. Re-Calibration and Data Analysis

The STSDAS **spec_polar** package contains tasks to examine, manipulate, and reprocess FOS spectropolarimetry observation datasets. Tasks are available to plot and examine both flux-calibrated spectra as well as polarization spectra that are derived from the flux-calibrated spectra. There are also tasks to average multiple datasets for a target either at the stage of flux-calibrated spectra or polarization spectra and to rebin polarization spectra in order to increase the signal-to-noise ratio. The following table summarizes the applicability of each task in the **spec_polar** package. More details and examples are available by typing “help spec_polar opt=sys”, or accessing the help files for specific routines in IRAF (see Table 4).

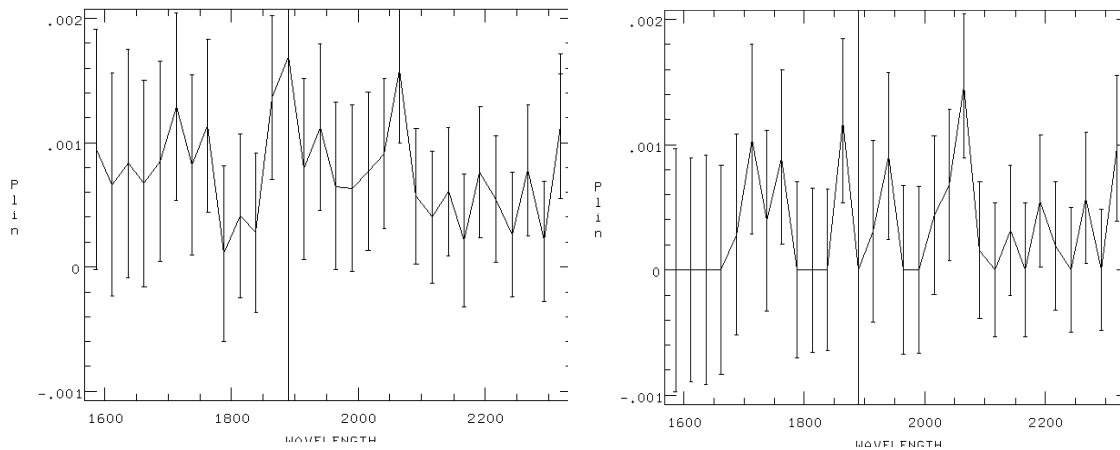
Table 4. Tasks in specpolar package

Task	Input	Output	Description
comparesets	c1h		Examine flux spectra
pcombine	c1h	c1h	Combine sets of flux spectra
calpolar	c1h	c3h	Compute polarization spectra, after manipulation by pcombine
plbias	c3h	c3h	Correct for bias in linear polarization
polave	c3h	c3h	Average c3h files
polbin	c3h	c3h	Rebin c3h file spectra
polcalc	c3h	c3h	Compute polarization spectra from Stokes IQUV
polnorm	c3h	c3h	Normalize Stokes QUV by I
polplot	c3h		Plot c3h file spectra

Biasing:

Of particular interest is the **plbias** routine. When Q and U are close to zero (the polarization signal is weak) an erroneous polarization could be produced because P is the sum of the squares of Q and U, which will always be positive. The **plbias** routine corrects the linear polarization spectra for the bias introduced in the calculation of P. See Figure 3 for an illustration with an observation of an unpolarized standard star, BD+28°4211. The data are corrected by replacing the linear polarization with $(p_l^2 - \sigma_p^2)^{1/2}$. This routine can be run at any time, on data fresh out of **calfos**, or after averaging with **polave** or binning with **polbin**. Note that the data should only be “biased” once, as the last step before final analysis. We recommend that you examine your data before and after biasing, if this step has a great effect on your results you will want to consider the detection level carefully (see section 4). We refer the reader to Simmons and Stewart (1985) for details in understanding the errors in polarization.

Figure 3: G190H polarization (unpolarized star, BD+28°4211) before (left) and after (right) biasing



Advanced techniques:

Note that the **polbin** routine allows for uneven binning of the data. If the flux varies strongly across your spectra, you may wish to increase the detection level of the polarization by using smaller bins where the flux is strong, and larger bins where the flux is weak. You can also bin to a given signal-to-noise level in the polarization.

Often data is taken in several different gratings and the desired output is the combination of these spectra—i.e., spectra are “stitched” together. The interaction between various spectrum stitching routines and the polarization routines is not good, so we recommend that you *first* reduce each grating’s polarization information and *then* stitch the spectra together.

Pitfalls:

Although FOS operation and calibration were quite robust, occasional operational problems could cause spurious polarization signals. You should always examine your raw data spectrum by spectrum, at each waveplate angle. This is particularly true if the reduced data shows something unusual, e.g., a weak signal where none was expected, or a strong polarization in the middle of a continuum region. Some common things to look for are cosmic ray hits and telescope “breathing.”

Model-based predictions of detector background due mostly to solar wind protons (“cosmic ray” events) was subtracted during pipeline processing, but you should check your .d0h data for spikes. You should edit these out by hand by changing the data quality value and reprocess the data to ensure good results.

As the telescope orbited the Earth, the mirror and other components cooled down and heated up and thus contracted and expanded slightly. This “breathing” could lead to some

de-focusing and possible wavelength-dependent light-loss, thereby inducing variations between the spectra in the POLSCAN series that would mimic real polarization effects. You should compare all the spectra to each other to see that they have the same general shape and slope. This problem was most acute pre-COSTAR.

4. FOS Polarimetry Calibration Accuracies

Wavelengths:

As with non-polarimetric observations, no concurrent WAVECAL exposure was routinely taken with polarimetry data, so the limiting accuracies of the default pipeline polarimetry wavelength calibration are the same as for the non-polarimetry case described in the *HST Data Handbook* (Vol. 2). Different dispersion relations are applied to the two pass directions. When the beams are combined, the pass 2 direction is simply shifted onto the wavelength grid of the pass 1 direction with no interpolation or resampling. The error in this arbitrary shift can be determined by simply comparing the output wavelengths for the two pass directions on a pixel-by-pixel basis. Wavelength calibration was based on a single epoch. Please refer to the wavelength calibration section of the *HST Data Handbook* (presently section 32.8) for updates to the wavelength calibration accuracy, which is currently quoted as up to 1 diode due to instrumental systemics.

Flatfields:

Polarimetry flatfields were produced via the often subjective, non-superflat, continuum-fitting technique. The errors inherent in this technique are of much less importance as polarimetry data are often binned heavily in analysis.

Fluxes:

Polarimetry flux calibration is performed with the FLX_CORR method and the white-dwarf absolute flux system. This has little effect on the derived values of Q and U as the influence of the sensitivity function divides out in the calculation of those quantities. No correction is made in the polarimetry FLX_CORR calibration for the influence of telescope focus or time-dependent photocathode sensitivity variation. These factors can cause an additional variable flux calibration underestimate of 0–15% for pre-COSTAR observations, but should not impact post-COSTAR calibration.

Pre-COSTAR Polarization:

Since the pre-COSTAR PSF overfilled all apertures, spacecraft jitter could impact some exposures in a POLSCAN sequence more than others, thereby introducing photometric effects that limited polarization measurement accuracy. For similar reasons, prior to the implementation of the onboard GIM correction, FOS polarimetry was not feasible. A

very few science program polarimetry observations were made in the period prior to implementation of the onboard GIM correction. Polarimetry accuracies from that time are potentially poor and are highly dependent on the actual, essentially indeterminate, GIM effects on each individual sub-exposure.

Following implementation of the onboard GIM correction, pre-COSTAR polarimetry accuracies were limited by the effects of residual GIM motion, FGW positioning, and jitter on the fraction of the s-curve of the large PSF that was recorded by the diode array. Visual inspection of pre-COSTAR calibrated polarimetry observations indicates that 1σ variations in these quantities produced scatter in total polarization of the order of 0.5% and occasionally was somewhat worse. The uncertainty in the retardation calibration also contributed a systematic instrumental polarization uncertainty equal to 2% (3% for G130H) of the linear polarization (see *FOS ISR 078*). The impact of photon statistical uncertainties always must be considered, but it can be minimized by appropriate binning of the data.

All reference files for the pre-COSTAR onboard GIM correction era have the USEAF-TER DATE of 8 June 1993.

Post-COSTAR Polarization:

The wavelength-dependent post-COSTAR instrumental polarization in Q varies from 0–3% over the FOS/BL 1600–3300Å spectral range and COSTAR-induced U varies from 0–0.5% over the same range. Panel a) of Figure 4 shows the magnitude of the COSTAR-induced instrumental polarization in high S/N observations of unpolarized spectrophotometric standard BD+28D4211 that have been combined into 64 bins. The discontinuity in U around 2300 Å is due to the break between the G190H and G270H gratings. Panel b) of Figure 4 shows a residual of $\sim 0.08\%$ in Q for the same binned spectrum after correction for the instrumental polarization with the algorithm that was discussed in section 2. Note that in the 1800–2100Å region where the waveplate retardation goes through 180 degrees, the limiting residual is $\sim 0.2\%$ (1σ). For bright objects, the polarization angles are known to within about ± 5 degrees (1σ). The post-COSTAR combined effects of residual GIM and spacecraft jitter do not produce polarization greater than 1%. Additional sources of error in polarization are due to the photon statistics of the observation and the error in the retardation calibration (2% of the linear polarization magnitudes—see *FOS ISR 078*). Post-COSTAR polarimetry observations made with only four polarizer positions (POLSCAN=4) contain an additional 0.4% uncertainty in Q, due to the inability to correct for COSTAR induced circular polarization. Note that polarimetry data for even very bright calibration sources typically must be binned in post-calibration data reduction in order to reach the levels of precision stated here.

Estimating Statistical Errors:

Photon counting statistics will be the dominant source of uncertainty in most observations. Following the formalism of *FOS ISR 078*, C_P is the sum of the photon counts at all

position angles in a polarimetry observation (sum of all groups in a POLSCAN series readout)

$$C_P = 0.5 T_P C_S \quad \text{Eq. 8}$$

where T_P is the transmission of the polarizer and C_S is the number of counts that would be expected in the same exposure time without the polarizer. Assuming a retardation, δ , for the waveplate, the uncertainty in the linear polarization, P_{LINEAR} , is

$$\sigma P_{\text{LINEAR}} = 2 \cdot \text{sqrt}(2.) (1 - \cos \delta)^{-1} (1. / C_P)^{0.5} \quad \text{Eq. 9}$$

the uncertainty in the plane of vibration, θ , is

$$\sigma_\theta = (90. / \pi) (P_{\text{LINEAR}})^{-1} (\sigma P_{\text{LINEAR}}) \quad \text{Eq. 10}$$

and the uncertainty in the circular polarization, P_{CIRC} , is

$$\sigma P_{\text{CIRC}} = (\text{sqrt}(2.) / \sin \delta) (1. / C_P)^{0.5} \quad \text{Eq. 11}$$

Table 6 presents results from equations 9 and 10 for retardation, δ , = 180 degrees.

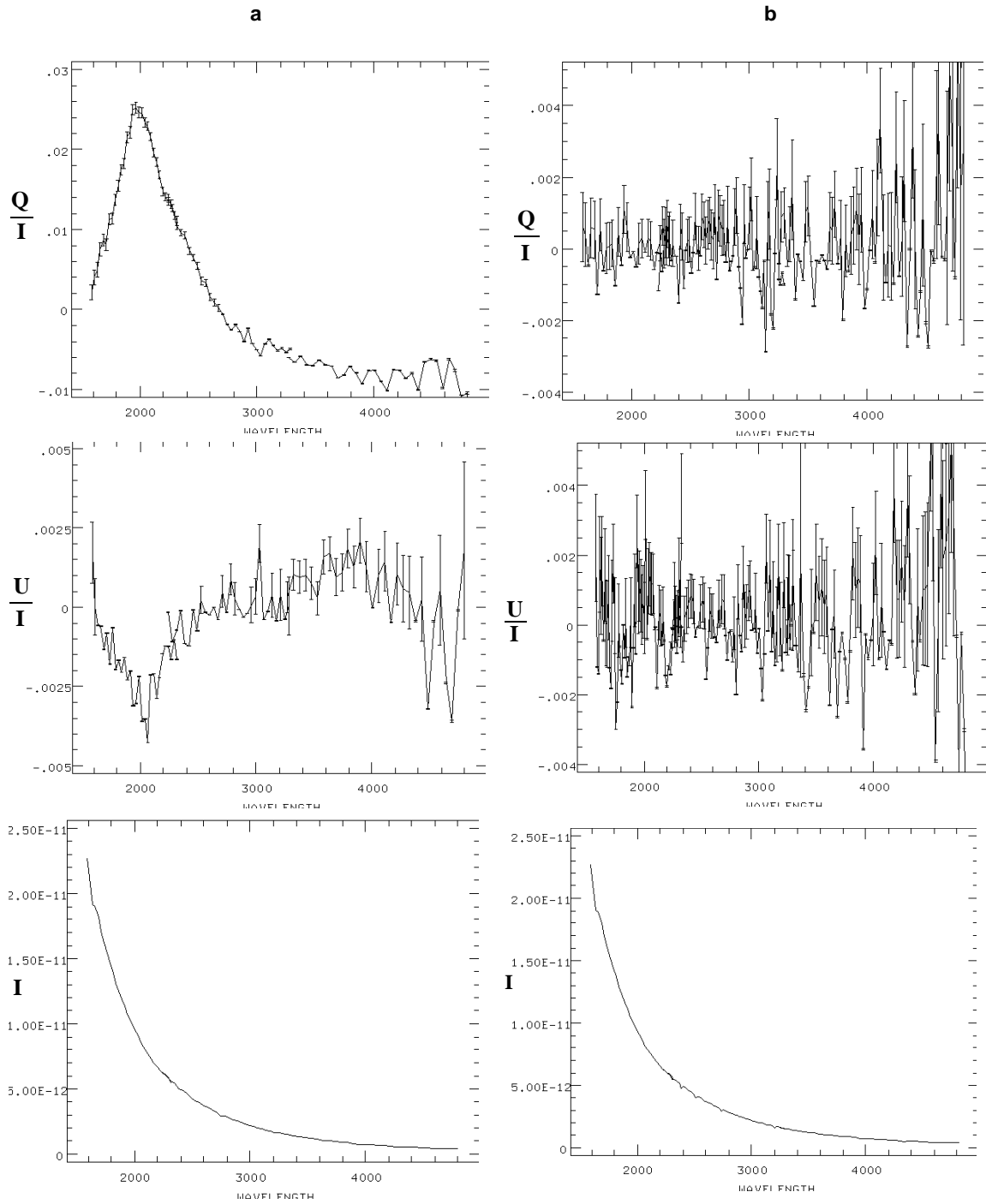
Table 5. Summary of limiting polarimetric sensitivities (1σ):

		Q/I	U/I	P_{CIRC}	P_{LINEAR}	Pos. angle θ
Pre-COSTAR		—	—	0.8%	0.3%	$\geq 2^\circ$
Post-COSTAR	POLSCAN=8,16	0.2%	0.2%	0.5%	0.5%	$\geq 2^\circ$
	POLSCAN=4	0.6%	—	—	0.7%	

Table 6. Linear polarization and position angle *formal* 1σ statistical errors for worst-case retardation, δ , = 180 degrees.

Total Counts	$P_{\text{LINEAR}} = 10\%$	$P_{\text{LINEAR}} = 1\%$
1600	$\sigma P_{\text{LINEAR}} = 3.54\%$	$\sigma P_{\text{LINEAR}} = 3.54\%$
	$\sigma_\theta = 10^\circ:1$	$\sigma_\theta = 101^\circ:1$
16,000	$\sigma P_{\text{LINEAR}} = 1.12\%$	$\sigma P_{\text{LINEAR}} = 1.12\%$
	$\sigma_\theta = 3^\circ:12$	$\sigma_\theta = 31^\circ:2$
160,000	$\sigma P_{\text{LINEAR}} = 0.35\%$	$\sigma P_{\text{LINEAR}} = 0.35\%$
	$\sigma_\theta = 1^\circ:01$	$\sigma_\theta = 10^\circ:1$

Figure 4: COSTAR induced polarization: spectra of an unpolarized standard star BD+28°4211 before (a) and after (b) correction.



5. COSTAR Polarization Correction

Allen (1995) recommends three corrections to the data. Following his notation, we call these UCORB, QCORB, and PHASB. From section 1 (last 5 paragraphs) we can determine that:

UCORB = U/I (from an unpolarized standard star),

QCORB = Q/I (from an unpolarized standard star), and

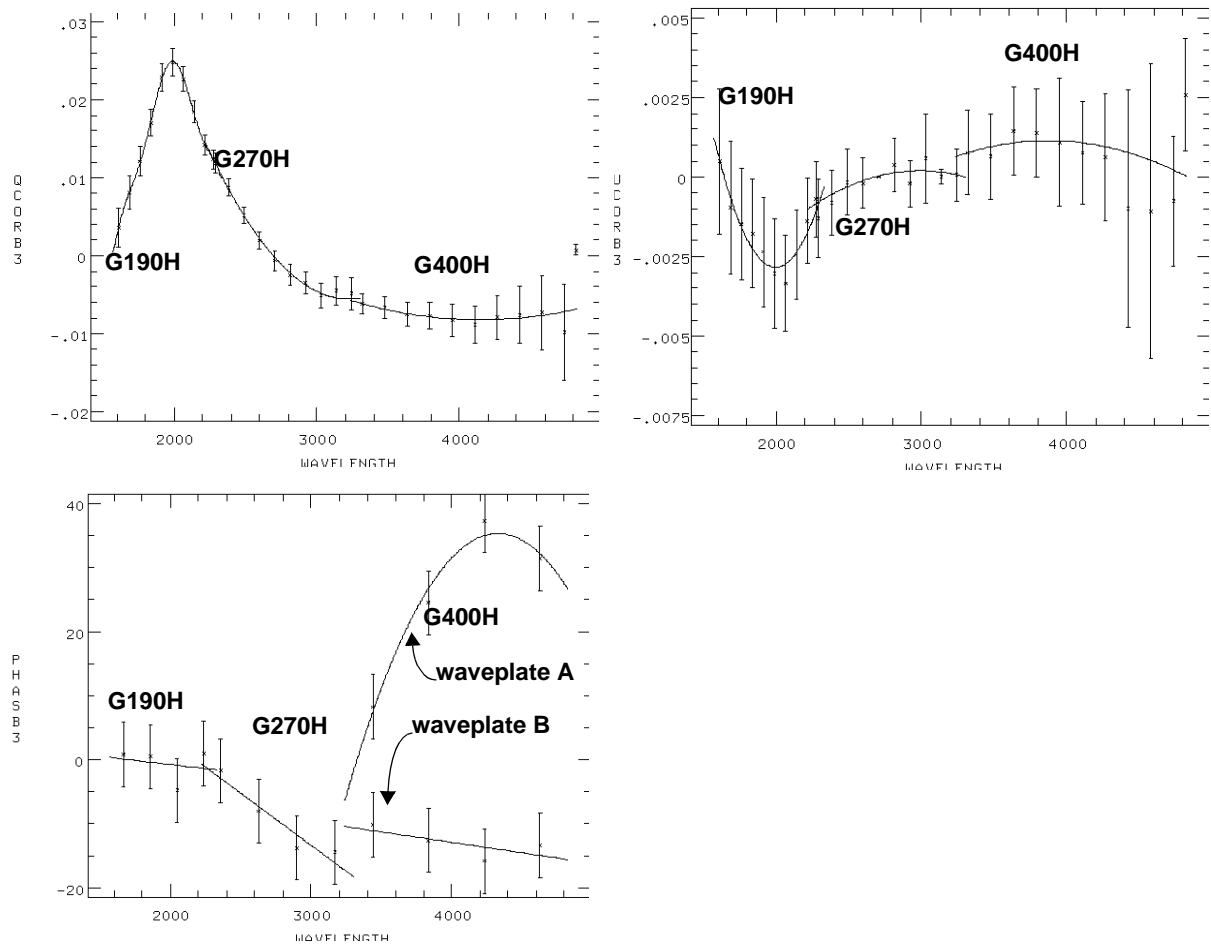
PHASB = $\arctan(V/U)$ (from a polarized star at 45 degrees from the axis).

FOS/BL observations of the unpolarized standard BD+28D4211 and the polarized standard BD+64D106 were made as part of program 6206—datasets y32006* for the former and y32004* (05 for H40 with the A waveplate) for the latter. These were processed to produce Stokes spectra with no COSTAR correction, and the above quantities derived. For each grating/waveplate, the derived values were saved as an `.r9h` image, the first three groups being QCORB for pass direction 1, pass direction 2, and the combined pass directions. Groups 4–6 are the corresponding UCORB values, and the last three groups are PHASB. An IRAF script to do this is given in appendix B. No corrections were derived for FOS/RD.

The data had to be dramatically smoothed and re-interpolated to get a usable SNR. For QCORB and UCORB, the 2064 pixels were averaged down to 11 bins, and for PHASB down to 4 bins. In addition, individual data points were adjusted so that a 3rd order (9th order for QCORB and G190H) Chebyshev interpolation (back to 2064 pixels) would fit the points well and not diverge at the ends of the range. Second-order interpolation was used for most of the PHASB values.

The results (Figure 5) agree well with Allen’s derived QCORB, UCORB, and PHASB values. The original observations of the polarized standard (BD+64D106) were made with the B waveplate, and so had to be repeated with the A waveplate. Fortunately this allowed a determination of the PHASB correction throughout the range of the correction supplied by Allen, and the agreement is very good. Both the A and B waveplate data for the G400H grating are shown in Figure 5. Allen (private communication, 1997) suggests that the PHASB correction is theoretically intractable and that the numbers he derived were consistent with zero shortward of 1600Å, and had an error of five degrees elsewhere. We use these errors in the last panel of Figure 5. These calibrations allow reliable polarimetric calibration throughout the wavelength range covered by the G190H, G270H, and G400H gratings. A small region ~40Å wide, centered at 1950Å, is still suspect, due to the retardation passing through 180 degrees there.

Figure 5: Post-COSTAR calibration figures. The interpolated values are plotted along with the binned data and propagated errors. The phase correction (bottom figure) shows both the A waveplate (upper curve) and B waveplate (lower curve) for the G400H. Only the former combination is calibrated post-COSTAR.



6. Summary of Re-archival of Re-calibrated FOS Polarimetry Data

All FOS polarimetry observations have been re-calibrated with the currently best-available reference files. These re-calibrated data have been delivered to the HST archive and are now available to any researcher as the default datasets.

A total of 26 pre-COSTAR programs including observations of 39 targets were updated. Nearly all of the pre-COSTAR scientific polarimetry program was carried out after the onboard GIM correction algorithm was installed. Of pre-COSTAR observations these programs will benefit the most from the re-calibration as improved calibration reference files (for observations after 8 June 1993) were delivered subsequent to pipeline processing of the original datasets.

For the post-COSTAR era, 11 programs including 35 targets were observed. None of the original observations as processed by the standard pipeline contained corrections for the post-COSTAR instrumental effects. *All* post-COSTAR FOS/BL data have been re-calibrated with completely updated reference files including the post-COSTAR instrumental polarization correction. Only three FOS/RD polarimetry science observations exist (programs 5684 and 5685), none of which has been calibrated for polarimetry or fluxes as the post-COSTAR FOS/RD flux and instrumental polarization calibrations are not defined. The FOS/RD observations have had all other normal calibrations applied, and .c1 files have been produced via the application of unity inverse sensitivity functions. No .c3 files will be archived nor will any be produced by normal calibration of these datasets as header parameter MOD_CORR is set to OMIT.

7. Conclusions and Recommendations

We wish to highlight several peculiarities and possibly non-obvious characteristics of FOS polarimetry data.

- In nearly all cases, the photon statistics of the observations are the limiting uncertainty.
- Only the 4.3 aperture was calibrated pre-COSTAR and only the 1.0 aperture was calibrated post-COSTAR.
- Circular polarization measurement is not possible for POLSCAN=4.
- Since the correction for COSTAR-induced instrumental polarization requires knowledge of the circular polarization, only data with POLSCAN=8 or 16 can be adequately corrected for the effects of the COSTAR mirrors.
- Pre-COSTAR researchers should always examine the individual POLSCAN spectra of the observations, particularly if more than one data readout is available for the target, to check for systematic errors. For example, routine calibration of pre-COSTAR data taken *before* the onboard GIM correction was implemented (nominally prior to 5 April 1993) attempts a model-derived GIM correction for the dispersion direction *only*. Although this helps with spectral resolution, the lack of any correction for image motion perpendicular to dispersion and, especially considering the large pre-COSTAR

PSF, probable light losses off the detector from one POLSCAN measurement to another can introduce serious systematic effects that mimic the effect of a polarized signal.

- As discussed above, the raw data should be carefully examined to determine if there are any effects of breathing or other instrumental artifacts. Also, the messages generated when **calfos** is run should be monitored carefully: if MOD_CORR is set to PERFORM, **calfos** will produce a .c3h file and will only warn you at run time of any problems. It is easy, for example, to specify the wrong PCP file for processing: **calfos** will produce an error message, but will happily fill the .r3h file with data that doesn't look too bad. The observer should generally use the IRAF **chcalpar** task to specify calibration file updates to the raw data headers.
- Note that since the post-COSTAR processing was added at a late date, the PCPHFILE header parameter will be appended to the header. It will not appear with the other calibration file parameters but may be found at the end of the header.
- Observers of weakly polarized objects should be careful about biasing: since the linear polarization is biased towards positive values, a correction should be made. Please review the "Data Analysis" section of this ISR.

8. References

- Allen, R.G., and Angel, J.R.P. (1982): "Performance of the Spectropolarimeter for the Space Telescope Faint Object Spectrograph", Proc. S.P.I.E. **331**, 259.
- Allen, R.G. (1995): "Status Report on Polarimetry with the FOS", in "Calibrating Hubble Space Telescope: Post Servicing Mission", ed. Koratkar and Leitherer, pp. 60-66.
- Allen, R.G., and Smith, P.S. (1992): "FOS Polarimetry Calibrations", FOS IDT report CAL/FOS-078.
- Allen, R.G., 1997, private communications.
- Keyes, T., ed., *HST Data Handbook*, volume II, 1997, STScI: Baltimore.
- Simmons, J.F.L., and Stewart, B.G. (1985): A and Ap, **141**, 100.

9. Appendix

A. IRAF Scripts for Calculating PCP Files

NOTE: this batch file assumes you have calibrated the data from program 6206 with a version of **calfos** that only does the pre-COSTAR processing, even though this data was taken post-COSTAR. In addition, all the data must be left in the instrument frame, and not rotated onto the sky frame. A special version of **calfos** which does this, is called **tstcal** and is available only at STScI and in the **testfos** environment of STSDAS. This file ends with a series of plots of PCPF files, each plot in interactive cursor mode. The user can examine the plot, print it if desired, and then type "q" to get the next plot. The end result is a series

of GEIS files that contain the QCORB, UCORB, and PHASB corrections for pass direction 1, pass direction 2, and pass directions 1 and 2 combined, and associated wavelength files. It is up to the user to interpolate these onto the diode scale and convert them into deliverable .r9h files. This will involve creating a nine-group image and converting it to real*8 (64 bit) numbers. For the calibration files, the former was done by editing the GCOUNT parameter, and the latter through use of the **chpixtype** IRAF routine.

```

imarf y3200607t.c3h[3] / y3200607t.c3h[1] foo
blkavg foo ucorb1a 205
imdel foo
imarf y3200607t.c3h[17] / y3200607t.c3h[15] foo
blkavg foo ucorb2a 205
imdel foo
imarf y3200607t.c3h[31] / y3200607t.c3h[29] foo
blkavg foo ucorb3a 205
imdel foo
imarf y3200607t.c3h[2] / y3200607t.c3h[1] foo
blkavg foo qcorb1a 205
imdel foo
imarf y3200607t.c3h[16] / y3200607t.c3h[15] foo
blkavg foo qcorb2a 205
imdel foo
imarf y3200607t.c3h[30] / y3200607t.c3h[29] foo
blkavg foo qcorb3a 205
imdel foo
imcalc y3200407t.c3h[4],y3200407t.c3h[3] foo "atan2(im1,im2) * -57.29578"
blkavg foo phasb1a 516
imdel foo
imcalc y3200407t.c3h[18],y3200407t.c3h[17] foo "atan2(im1,im2) * -57.29578"
blkavg foo phasb2a 516
imdel foo
imcalc y3200407t.c3h[32],y3200407t.c3h[31] foo "atan2(im1,im2) * -57.29578"
blkavg foo phasb3a 516
imdel foo
imarf y3200608t.c3h[3] / y3200608t.c3h[1] foo
blkavg foo ucorb1b 205
imdel foo
imarf y3200608t.c3h[17] / y3200608t.c3h[15] foo
blkavg foo ucorb2b 205
imdel foo
imarf y3200608t.c3h[31] / y3200608t.c3h[29] foo
blkavg foo ucorb3b 205
imdel foo
imarf y3200608t.c3h[2] / y3200608t.c3h[1] foo
blkavg foo qcorb1b 205
imdel foo
imarf y3200608t.c3h[16] / y3200608t.c3h[15] foo
blkavg foo qcorb2b 205
imdel foo
imarf y3200608t.c3h[30] / y3200608t.c3h[29] foo
blkavg foo qcorb3b 205
imdel foo
imcalc y3200408t.c3h[4],y3200408t.c3h[3] foo "atan2(im1,im2) * -57.29578"
blkavg foo phasb1b 516
imdel foo
imcalc y3200408t.c3h[18],y3200408t.c3h[17] foo "atan2(im1,im2) * -57.29578"
blkavg foo phasb2b 516
imdel foo
imcalc y3200408t.c3h[32],y3200408t.c3h[31] foo "atan2(im1,im2) * -57.29578"
blkavg foo phasb3b 516
imdel foo
blkavg y3200607t.c0h[1] lamh19 205
blkavg y3200407t.c0h[1] slamh19 516
imcalc ucorb1a,ucorb1b ucorb1h19 "(im1 + im2) / 2."
imcalc ucorb2a,ucorb2b ucorb2h19 "(im1 + im2) / 2."
imcalc ucorb3a,ucorb3b ucorb3h19 "(im1 + im2) / 2."
imcalc qcorb1a,qcorb1b qcorb1h19 "(im1 + im2) / 2."
imcalc qcorb2a,qcorb2b qcorb2h19 "(im1 + im2) / 2."
imcalc qcorb3a,qcorb3b qcorb3h19 "(im1 + im2) / 2."
imcalc phasb1a,phasb1b phasb1h19 "(im1 + im2) / 2."
imcalc phasb2a,phasb2b phasb2h19 "(im1 + im2) / 2."
imcalc phasb3a,phasb3b phasb3h19 "(im1 + im2) / 2."
imarf y3200609t.c3h[3] / y3200609t.c3h[1] foo
blkavg foo ucorb1c 205
imdel foo
imarf y3200609t.c3h[17] / y3200609t.c3h[15] foo
blkavg foo ucorb2c 205
imdel foo
imarf y3200609t.c3h[31] / y3200609t.c3h[29] foo
blkavg foo ucorb3c 205
imdel foo
imarf y3200609t.c3h[2] / y3200609t.c3h[1] foo
blkavg foo qcorb1c 205
imdel foo

```

```

imar y3200609t.c3h[16] / y3200609t.c3h[15] foo
blkavg foo qcorb2c 205
imdel foo
imar y3200609t.c3h[30] / y3200609t.c3h[29] foo
blkavg foo qcorb3c 205
imdel foo
imcalc y3200409t.c3h[4],y3200409t.c3h[3] foo "atan2(im1,im2) * -57.29578"
blkavg foo phasb1c 516
imdel foo
imcalc y3200409t.c3h[18],y3200409t.c3h[17] foo "atan2(im1,im2) * -57.29578"
blkavg foo phasb2c 516
imdel foo
imcalc y3200409t.c3h[32],y3200409t.c3h[31] foo "atan2(im1,im2) * -57.29578"
blkavg foo phasb3c 516
imdel foo
imar y320060at.c3h[3] / y320060at.c3h[1] foo
blkavg foo ucorb1d 205
imdel foo
imar y320060at.c3h[17] / y320060at.c3h[15] foo
blkavg foo ucorb2d 205
imdel foo
imar y320060at.c3h[31] / y320060at.c3h[29] foo
blkavg foo ucorb3d 205
imdel foo
imar y320060at.c3h[2] / y320060at.c3h[1] foo
blkavg foo qcorb1d 205
imdel foo
imar y320060at.c3h[16] / y320060at.c3h[15] foo
blkavg foo qcorb2d 205
imdel foo
imar y320060at.c3h[30] / y320060at.c3h[29] foo
blkavg foo qcorb3d 205
imdel foo
imcalc y320040at.c3h[4],y320040at.c3h[3] foo "atan2(im1,im2) * -57.29578"
blkavg foo phasb1d 516
imdel foo
imcalc y320040at.c3h[18],y320040at.c3h[17] foo "atan2(im1,im2) * -57.29578"
blkavg foo phasb2d 516
imdel foo
imcalc y320040at.c3h[32],y320040at.c3h[31] foo "atan2(im1,im2) * -57.29578"
blkavg foo phasb3d 516
imdel foo
blkavg y3200609t.c0h[1] lamh27 205
blkavg y3200409t.c0h[1] slamh27 516
imcalc ucorb1c,ucorb1d ucorb1h27 "(im1 + im2) / 2."
imcalc ucorb2c,ucorb2d ucorb2h27 "(im1 + im2) / 2."
imcalc ucorb3c,ucorb3d ucorb3h27 "(im1 + im2) / 2."
imcalc qcorb1c,qcorb1d qcorb1h27 "(im1 + im2) / 2."
imcalc qcorb2c,qcorb2d qcorb2h27 "(im1 + im2) / 2."
imcalc qcorb3c,qcorb3d qcorb3h27 "(im1 + im2) / 2."
imcalc phasb1c,phasb1d phasb1h27 "(im1 + im2) / 2."
imcalc phasb2c,phasb2d phasb2h27 "(im1 + im2) / 2."
imcalc phasb3c,phasb3d phasb3h27 "(im1 + im2) / 2."
imar y3200605t.c3h[3] / y3200605t.c3h[1] foo
blkavg foo ucorb1e 205
imdel foo
imar y3200605t.c3h[17] / y3200605t.c3h[15] foo
blkavg foo ucorb2e 205
imdel foo
imar y3200605t.c3h[31] / y3200605t.c3h[29] foo
blkavg foo ucorb3e 205
imdel foo
imar y3200605t.c3h[2] / y3200605t.c3h[1] foo
blkavg foo qcorb1e 205
imdel foo
imar y3200605t.c3h[16] / y3200605t.c3h[15] foo
blkavg foo qcorb2e 205
imdel foo
imar y3200605t.c3h[30] / y3200605t.c3h[29] foo
blkavg foo qcorb3e 205
imdel foo
imcalc y3200505t.c3h[4],y3200505t.c3h[3] foo "atan2(im1,im2) * -57.29578"
blkavg foo phasb1e 516
imdel foo
imcalc y3200505t.c3h[18],y3200505t.c3h[17] foo "atan2(im1,im2) * -57.29578"
blkavg foo phasb2e 516
imdel foo
imcalc y3200505t.c3h[32],y3200505t.c3h[31] foo "atan2(im1,im2) * -57.29578"
blkavg foo phasb3e 516
imdel foo
imar y3200606t.c3h[3] / y3200606t.c3h[1] foo
blkavg foo ucorb1f 205
imdel foo
imar y3200606t.c3h[17] / y3200606t.c3h[15] foo
blkavg foo ucorb2f 205
imdel foo
imar y3200606t.c3h[31] / y3200606t.c3h[29] foo
blkavg foo ucorb3f 205
imdel foo
imar y3200606t.c3h[2] / y3200606t.c3h[1] foo
blkavg foo qcorb1f 205
imdel foo

```

```

imar y3200606t.c3h[16] / y3200606t.c3h[15] foo
blkavg foo qcorb2f 205
imdel foo
imar y3200606t.c3h[30] / y3200606t.c3h[29] foo
blkavg foo qcorb3f 205
imdel foo
imcalc y3200506t.c3h[4],y3200506t.c3h[3] foo "atan2(im1,im2) * -57.29578"
blkavg foo phasb1f 516
imdel foo
imcalc y3200506t.c3h[18],y3200506t.c3h[17] foo "atan2(im1,im2) * -57.29578"
blkavg foo phasb2f 516
imdel foo
imcalc y3200506t.c3h[32],y3200506t.c3h[31] foo "atan2(im1,im2) * -57.29578"
blkavg foo phasb3f 516
imdel foo
blkavg y3200605t.c0h[1] lamh40 205
blkavg y3200505t.c0h[1] slamh40 516
imcalc ucorb1e,ucorb1f ucorb1h40 "(im1 + im2) / 2."
imcalc ucorb2e,ucorb2f ucorb2h40 "(im1 + im2) / 2."
imcalc ucorb3e,ucorb3f ucorb3h40 "(im1 + im2) / 2."
imcalc qcorb1e,qcorb1f qcorb1h40 "(im1 + im2) / 2."
imcalc qcorb2e,qcorb2f qcorb2h40 "(im1 + im2) / 2."
imcalc qcorb3e,qcorb3f qcorb3h40 "(im1 + im2) / 2."
imcalc phasb1e,phasb1f phasb1h40 "(im1 + im2) / 2."
imcalc phasb2e,phasb2f phasb2h40 "(im1 + im2) / 2."
imcalc phasb3e,phasb3f phasb3h40 "(im1 + im2) / 2."
fwplot ucorb1h19 wave=lamh19 ylabel="UCORB1" append=no pointmode=no wl=1500 wr=4900 wb=-0.005 wt=0.002
fwplot ucorb1h27 wave=lamh27 append=yes pointmode=no
fwplot ucorb1h40 wave=lamh40 append=yes pointmode=no
=gcur
fwplot ucorb2h19 wave=lamh19 ylabel="UCORB2" append=no pointmode=no wl=1500 wr=4900 wb=-0.005 wt=0.002
fwplot ucorb2h27 wave=lamh27 append=yes pointmode=no
fwplot ucorb2h40 wave=lamh40 append=yes pointmode=no
=gcur
fwplot ucorb3h19 wave=lamh19 ylabel="UCORB3" append=no pointmode=no wl=1500 wr=4900 wb=-0.005 wt=0.002
fwplot ucorb3h27 wave=lamh27 append=yes pointmode=no
fwplot ucorb3h40 wave=lamh40 append=yes pointmode=no
=gcur
fwplot qcorb1h19 wave=lamh19 ylabel="QCORB1" append=no pointmode=no wl=1500 wr=4900 wb=-0.015 wt=0.03
fwplot qcorb1h27 wave=lamh27 append=yes pointmode=no
fwplot qcorb1h40 wave=lamh40 append=yes pointmode=no
=gcur
fwplot qcorb2h19 wave=lamh19 ylabel="QCORB2" append=no pointmode=no wl=1500 wr=4900 wb=-0.015 wt=0.03
fwplot qcorb2h27 wave=lamh27 append=yes pointmode=no
fwplot qcorb2h40 wave=lamh40 append=yes pointmode=no
=gcur
fwplot qcorb3h19 wave=lamh19 ylabel="QCORB3" append=no pointmode=no wl=1500 wr=4900 wb=-0.015 wt=0.03
fwplot qcorb3h27 wave=lamh27 append=yes pointmode=no
fwplot qcorb3h40 wave=lamh40 append=yes pointmode=no
=gcur
fwplot phasb1h19 wave=slamh19 ylabel="PHASB1" append=no pointmode=no wl=1500 wr=4900 wb=-20 wt=30
fwplot phasb1h27 wave=slamh27 append=yes pointmode=no
fwplot phasb1h40 wave=slamh40 append=yes pointmode=no
=gcur
fwplot phasb2h19 wave=slamh19 ylabel="PHASB2" append=no pointmode=no wl=1500 wr=4900 wb=-20 wt=30
fwplot phasb2h27 wave=slamh27 append=yes pointmode=no
fwplot phasb2h40 wave=slamh40 append=yes pointmode=no
=gcur
fwplot phasb3h19 wave=slamh19 ylabel="PHASB3" append=no pointmode=no wl=1500 wr=4900 wb=-20 wt=30
fwplot phasb3h27 wave=slamh27 append=yes pointmode=no
fwplot phasb3h40 wave=slamh40 append=yes pointmode=no
=gcur

```